11-18-2016

Phytochrome B integrates light and temperature signals in Arabidopsis

Martina Legris

Cornelia Klose

E Sethe Burgie

Cecilia Costigliolo Rojas Rojas

Maximiliano Neme

See next page for additional authors

Title:

Phytochrome B integrates light and temperature signals in Arabidopsis

Authors: Martina Legris[1], Cornelia Klose[2,†], E. Sethe Burgie[3,†], Cecilia Costigliolo[1,†], Maximiliano Neme[1], Andreas Hiltbrunner[2,4], Philip A. Wigge[5], Eberhard Schäfer[2,4,‡], Richard D. Vierstra[3,‡], Jorge J. Casal[1,6,*]

Affiliations:

[1]Fundación Instituto Leloir, Instituto de Investigaciones Bioquímicas de Buenos Aires–CONICET, 1405 Buenos Aires, Argentina

[2]Institut für Biologie II, University of Freiburg, Schaenzlestr. 1, D-79104 Freiburg.

[3]Department of Biology, Washington University in St. Louis, Campus Box 1137, One Brookings Drive, St. Louis, MO 63130, USA

[4]BIOSS Centre for Biological Signaling Studies, University of Freiburg, Schaenzlestr. 18, 79104 Freiburg, Germany

[5]Sainsbury Laboratory, Cambridge University, 47 Bateman St. Cambridge CB2 1LR, UK

[6]IFEVA, Facultad de Agronomía, Universidad de Buenos Aires and CONICET, Av. San Martín 4453, 1417 Buenos Aires, Argentina.

*Correspondence to: casal@ifeva.edu.ar.

[†]These authors contributed equally.

[‡]These authors contributed equally.

Abstract:

Ambient temperature regulates many aspects of plant growth and development but its sensors are unknown. Here, we demonstrate that the phytochrome B (phyB) photoreceptor participates in temperature perception through its temperature-dependent reversion from the active Pfr state to the inactive Pr state. Increased rates of thermal reversion upon exposing Arabidopsis seedlings to warm environments reduce both the abundance of the biologically active Pfr-Pfr dimer pool of phyB and the size of the associated nuclear bodies, even in daylight. Mathematical analysis of stem growth for seedlings expressing wild-type phyB or thermally stable variants under various combinations of light and temperature revealed that phyB is physiologically responsive to both signals. We therefore propose that in addition to its photoreceptor functions, phyB is a temperature sensor in plants.

One Sentence Summary:

Activity of the red-light photoreceptor phytochrome B is modulated by temperature.

Main Text:

Plants have the capacity to adjust their growth and development in response to light and temperature cues (*1*). Temperature sensing helps plants determine when to germinate, adjust their body plan to protect themselves from adverse temperatures, and flower. Warm temperatures as well as reduced light resulting from vegetative shade promote stem growth, enabling seedlings to avoid heat stress and canopy shade from neighboring plants. Whereas light perception is driven by a collection of identified photoreceptors, including the red/far-red light-absorbing phytochromes, the blue/UV-A light-absorbing cryptochromes, phototropins, and members of the Zeitlupe family, and the UV-B-absorbing UVR8 (*2*), temperature sensors remain to be established (*3*). Finding the identit(ies) of temperature sensors would be of particular relevance in the context of climate change (*4*).

Phytochrome B (phyB) is the main photoreceptor controlling growth in Arabidopsis seedlings exposed to different shade conditions (*5*). Like others in the phytochrome family, phyB is a homodimeric chromoprotein with each subunit harboring a covalently bound phytochromobilin chromophore. phyB exists in two photo-interconvertible forms, a red-light absorbing Pr state that is biologically inactive and a far-red light-absorbing Pfr state that is biologically active (*6, 7*). Whereas Pr arises upon assembly with the bilin, formation of Pfr requires light and its levels are strongly influenced by the red/far-red light ratio. Consequently, because red light is absorbed by photosynthetic pigments, shade light from neighboring vegetation has a strong impact on Pfr levels by reducing this ratio (*8*). phyB Pfr also spontaneously reverts back to Pr in a light-independent reaction called thermal reversion (*9–11*). Traditionally, thermal reversion was assumed to be too slow relative to the light reactions to

affect the Pfr status of phyB even under moderate irradiances found in natural environments, but two observations contradict this view. First, the formation of phyB nuclear bodies, which reflects the status of Pfr, is affected by light up to irradiances much higher than expected if thermal reversion were slow (*12*). Second, it is now clear that thermal reversion occurs in two steps. Although the first step, from the Pfr:Pfr homodimer (D2) to the Pfr:Pr heterodimer (D1) is slow (kr2), the second step, from the Pfr:Pr heterodimer to the Pr:Pr homodimer (D0), is almost two orders of magnitude faster (kr1) (*11*) (Fig 1A).

Physiologically relevant temperatures could change the magnitude of kr1 and consequently affect Pfr and D2 levels even under illumination (Fig 1A). To test this hypothesis, we used *in vitro* and *in vivo* spectroscopy and analysis of phyB nuclear bodies by confocal microscopy. For the first of these approaches we produced recombinant full-length phyB bearing its phytochromobilin chromophore. When irradiated under continuous red light, the *in vitro* absorbance at 725 nm, reached lower values at higher temperatures, indicative of reduced steady state levels of Pfr (Fig. 1B, C). We calculated the differences between the steady-state absorbance spectra in darkness and continuous red light (Δ absorbance). The amplitude between the maximum and minimum peaks of Δ absorbance, which represents the amount of Pfr, strongly decreased between 10 and 30 °C (Fig, 1D, E). This characteristic of phyB differs from the typical behavior of enzymes, which exhibit increased activity over the same temperature range (*13*).

We also measured by *in vivo* spectroscopy the steady-state levels of phyB Pfr in seedlings irradiated with continuous red or white light at different temperatures (applied only during the irradiation). Increasing temperatures reduced both the total pool of Pfr and that of D2 (Fig. 1F, S1), which is considered to be the physiologically-relevant species for phyB (*11*). Using these data, we determined kr1, which increased with temperature (Fig. 1G).

phyB nuclear body formation increases with irradiance and red/far-red light ratio (*12*, *14*) because it depends on D2 (*11*). As a proxy for temperature impact on D2 we used the difference in nuclear body formation in lines of the *phyB-9* null mutant rescued with unmodified phyB (phyB-YFP) or either of two chromophore pocket mutants that suppress Pfr thermal reversion *in vitro* with little to no effect on photoconversion (phyB^{Y361F}-YFP and phyB^{R582A}-YFP) (*15*, *16*). De-etiolated (green) seedlings were transferred to the different light conditions (irradiances, red/far-red light ratios) representative of unfiltered sunlight, canopy shade or cloudy days, in combination with different temperatures applied only during the light treatments (Fig. S2). The nuclear body size of phyB^{Y361F}-YFP and phyB^{R582A}-YFP was not significantly impacted by irradiance (Fig. S3) and strongly affected by the red/far-red ratio (Fig. S4). This is consistent with the notion that irradiance responses depend on kr1 and kr2 (*11*), which are affected in the mutants. The size of phyB nuclear bodies varied quadratically with temperature and was largest at ~20 °C (Fig. 2A, Fig. S5). We tested the hypothesis that the negative phase of this response to temperature is the manifestation of enhanced thermal reversion reducing D2. Toward this aim we modeled the average size of the phyB^{Y361F}-YFP and phyB^{R582A}-YFP nuclear bodies (Tables S1, S2) as a function of both D2 (*11*) and temperature effects not mediated by changes in D2 (Fig. S6). Then we used this restricted model to predict D2 levels from phyB nuclear body sizes in wild-type lines (Fig. 2B). Fig. 2C shows the difference between the apparent log D2 in wild-type and the log D2 of phyB^{Y361F} and phyB^{R582A} in the same light condition (difference averaged for all light conditions). The results indicate that high temperatures decrease the apparent D2 for the wild-type phyB under a wide range of light conditions.

By using the three approaches above, we showed that the activity of phyB decreases with increasing temperature (Fig. 1-2) suggesting two possible biological outcomes. One is that

downstream changes in phyB signaling compensate for the temperature effect. The circadian clock provides an example of temperature compensation (*17*). The other is that phyB perception of temperature cues controls the physiological output. A prediction of the latter hypothesis is that phyB activity (D2) should similarly affect growth independently of whether it is altered by light, temperature, or mutations that stabilize phyB. To test this prediction, we cultivated Arabidopsis seedlings (including phyB genetic variants) at the same irradiance and temperature, sorted them to the different light and temperature environments (Fig. S2), and modeled growth under these conditions (Table S3) as a function of D2.

The growth responses to temperature (Fig. S7) and light (*18*) are not exclusively mediated by phyB (D2). Thus, we built the model in two steps, first fitting univariate submodels describing the relationship between growth and the individual factors (D2, temperature effects not mediated by changes in D2, activity of other photo-sensory receptors) and then combining those components in the final model. To quantify the contribution of D2 (Fig. S8), we used growth at 30°C (no low-temperature inhibition of growth, Fig. S9) of all genotypes, including the stabilized phyB variants and the *phyB* null mutant (D2= 0). To quantify the effects of temperature not mediated by changes in D2 (Fig. S9B), we used the *phyB* mutant (no phyB-mediated inhibition) at 1 μmol . m^{-2} . s^{-1} (at this irradiance, at 30 °C growth is maximal, indicating that other photoreceptors do not make a strong contribution). To quantify the contribution of other photoreceptors (Fig. S10), we used the *phyB* mutant (no phyB-mediated inhibition) at a range of irradiances at 30 °C (no low-temperature growth inhibition). The only statistically significant interaction among these terms was between D2 and temperature effects not mediated by changes in D2 (Table S4). Therefore, in the final model, growth was inversely related to terms representing the actions of D2, low temperatures (not mediated by changes in

D2), other photo-sensory receptors and the synergistic interaction between D2 and low temperature (not mediated by changes in D2).

We then fitted growth for all the 200 light-temperature-genotype combinations to the model. The relationship between observed and predicted data showed no systematic deviation from the 1:1 correlation for the different light (Fig. 3A), temperature (Fig. 3B) or genetic variants with altered Pfr stability (Fig. 3C). Predicted data were obtained with D2 values affected by light, temperature and genotype. To test the significance of temperature effects mediated by changes in the status of phyB, we recalculated growth by using D2 modified by light and genotype but not by temperature (constant 10°C). This adjustment reduced the growth model goodness of fit (Fig. 3B, inset), indicating that the contribution of phyB-mediated temperature effects on growth is statistically significant and should not be neglected. Because we estimated the effect of D2 using data from a single temperature (Fig. S8), our growth model is not based on the assumption that D2 changes with temperature, thus providing confidence that the latter conclusion is genuine.

We used the growth model to compare the contribution of each of the three temperature-dependent terms to the inhibition of growth by low temperatures. phyB-mediated effects of temperature contribute to the overall temperature response (Fig. 3D). The effects were large at low irradiances, decreased with intermediate irradiances (light reactions become increasingly important) and increased again at higher irradiances because now D2 impacts growth more strongly.

Phytochromes were discovered and have been studied based on their roles as light receptors in plants (*6*, *7*). However, our observations that temperature alters the amount of D2 for phyB (Fig. 1-2) and its physiological output in a manner similar to light (Fig. 3) indicate that

phyB should also be defined as a temperature cue receptor. Interestingly, phyB requires light to comply with this temperature function by needing light to initially generate the unstable but bioactive Pfr state. Temperature affects the Pfr status of phyB mainly via kr1 in the light (Fig. 1) and via kr2 during the night (*19*). Receptors are often activated by their ligands; although phyB is activated by red light it is inactivated by far-red light and high temperatures. This combination of light and temperature perception would serve to integrate the signals controlling photo- and thermo-morphogenesis in ways that optimize the growth of plants exposed to a wide range of environments.

References and Notes:

1. J. J. Casal, C. Fankhauser, G. Coupland, M. A. Blázquez, *Trends Plant Sci.* **9**, 309–314 (2004).
2. V. C. Galvão, C. Fankhauser, *Curr. Opin. Neurobiol.* **34**, 46–53 (2015).
3. M. Quint *et al.*, *Nat. Plants*. **2**, 15190 (2016).
4. D. S. Battisti, R. L. Naylor, *Science*. **323**, 240–4 (2009).
5. J. J. Casal, *Annu. Rev. Plant Biol.* **64**, 403–27 (2013).
6. P. H. Quail *et al.*, *Science.* **268**, 675–680 (1995).
7. E. S. Burgie, R. D. Vierstra, *Plant Cell*. **26**, 4568–83 (2014).
8. M. G. Holmes, H. Smith, *Photochem. Photobiol.* **25**, 539–545 (1977).
9. U. Sweere *et al.*, *Science.* **294**, 1108–1111 (2001).
10. É. Ádám *et al.*, *PLoS One*. **6**, e27250 (2011).
11. C. Klose *et al.*, *Nat. Plants*. **1**, 15090 (2015).
12. S. A. Trupkin, M. Legris, A. S. Buchovsky, M. B. Tolava Rivero, J. J. Casal, *Plant Physiol.* **165**, 1698–1708 (2014).
13. M. E. Salvucci, K. W. Osteryoung, S. J. Crafts-Brandner, E. Vierling, *Plant Physiol.* **127**, 1053–1064 (2001).
14. E. K. van Buskirk, P. V Decker, M. Chen, *Plant Physiol.* **158**, 52–60 (2012).
15. J. Zhang, R. J. Stankey, R. D. Vierstra, *Plant Physiol.* **161**, 1445–1457 (2013).
16. E. S. Burgie, A. N. Bussell, J. M. Walker, K. Dubiel, R. D. Vierstra, *Proc. Natl. Acad. Sci. U. S. A.* **111**, 10179–84 (2014).
17. P. A. Salomé, D. Weigel, C. R. McClung, *Plant Cell*. **22**, 3650–61 (2010).
18. R. Sellaro *et al.*, *Plant Physiol.* **154**, 401–409 (2010).
19. J.-H. Jung *et al.*, *Science aaf6005* (2016).

Acknowledgments: We thank Filippo Venezia (University of Freiburg) for his valuable help with the analytical equations. Supported by *Agencia Nacional de Promoción Científica y Tecnológica* (grants no. PICT 2012-1396 and PICT 2013-1444 to JJC), Alexander von Humboldt-Foundation (JJC), *Universidad de Buenos Aires* (grant no.20020100100437 to JJC), *Fundación Rene Baron* (JJC), the Excellence Initiative of the German Federal and State Governments (EXC 294, project C 20 to ES and AH), the German Research Foundation (DFG; SCHA 303/16-1 and HI 1369/5-1 to ES and AH), and the US National Science Foundation (MCB-1329956 to RDV). R.D.V and E.S.B. and the University of Wisconsin-Madison have filed patent application P140220US02 that relates to the use of mutants phyB^{Y361F} and phyB^{R582A} in agriculture. Supplement contains additional data.

Supplementary Materials

Materials and Methods

Figs. S1 to S11

Table S1 to S4

References (20–26)

Fig. 1. The status of phyB responds to light and temperature. (**A**) Three stage model of phyB (*11*). Our working hypothesis is that D2 integrates light cues (via k1 and k2) and temperature cues (via kr2 and mainly kr1). (**B-E**) Warm temperatures reduce Pfr levels of full-length recombinant phyB exposed *in vitro* to 1 (B, D) or 5.1 (C, E) μmol . m^{-2} . s^{-1} of continuous red light. (B, C) Absorbance kinetics (maximal absorption decreased with temperature, $P < 0.05$). (D, E) Difference in absorbance (Δ absorbance) in samples incubated in darkness or exposed to continuous red light to reach a steady state. The difference between Δ absorbance at 665 and 725 nm decreased with temperature ($P < 0.01$). (**F**) Warm temperatures reduce the levels of Pfr and D2 *in vivo* measured in *phyA* mutant seedlings overexpressing phyB (*9*) exposed to 1 μmol . m^{-2} . s^{-1} red light. Means ±SE of 3 biological replicates. (**G**) Warm temperatures increase kr1 (calculated from (F), $P < 0.001$).

Fig. 2. phyB nuclear bodies respond to light and temperature. (**A**) Dual response of phyB-YFP nuclear bodies to temperature (white light, 10 μmol . m^{-2} . s^{-1}, bar = 5μm). (**B**) Estimation of D2 in the wild type by using its average phyB nuclear body size (NB) as input in the model relating NB to D2 in lines expressing stabilized phyB ($phyB^{Y361F}$-YFP and $phyB^{R582A}$-YFP). (**C**) Impact of temperature on D2. Difference in log-transformed D2 averaged for 5-11 conditions (±SE) covering a wide range of irradiances and red/far-red ratios (temperature effect: $P < 0.05$).

Fig. 3. phyB mediates growth responses to light and temperature. (**A-C**) Observed values of hypocotyl growth (*G*) in white light-grown seedlings of 8 genotypes exposed to 25 combinations of irradiance and temperature versus the values predicted by the growth model. The different irradiances (A), temperatures (B) and genotypes (C) are color coded to show that the relationship

between observed and predicted values is not biased for any of these factors (within the range tested here). Col: Columbia wild type, *phyB*: phyB null mutant, phyB, phyB^{Y361F}, and phyB^{R582A}: transgenic lines expressing wild-type or mutated phyB in the *phyB* null mutant background. B, inset: The goodness of fit of the model (Pearson's chi-squared test) is seriously deteriorated when temperature effects on D2 are not incorporated (both versions of the model have the same number of parameters). (**D**) Contribution to the inhibition of growth of each one of the three temperature-dependent terms of the growth model. Uppermost line: horizontal base line of no low temperature effects (*G* incorporating only light effects at 30 °C). Downwards, the lines indicate *G* calculations successively incorporating the phyB-dependent temperature effects, the phyB-temperature interaction and the phyB-independent temperature effect. The colored areas highlight the contribution of each additional term incorporated in the calculations.

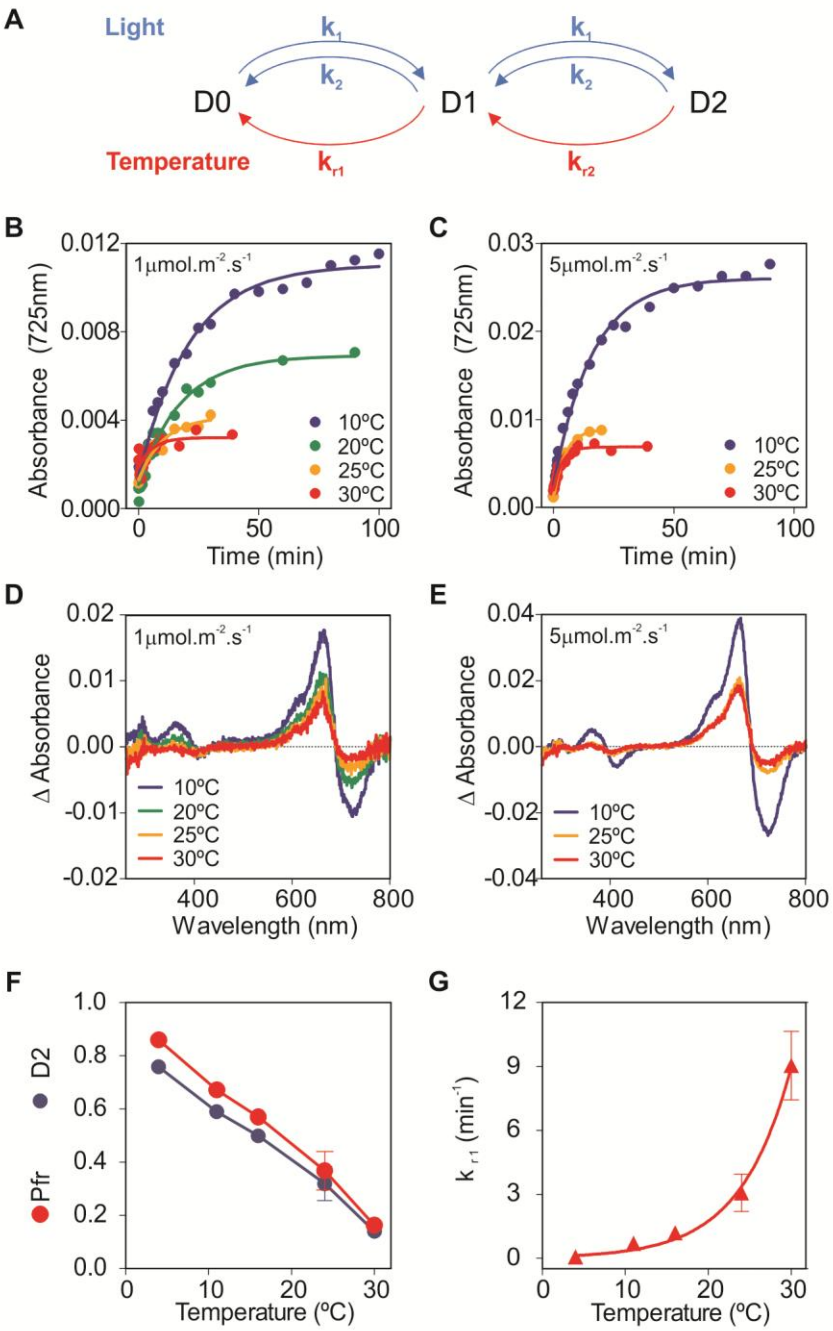
A
Light
k1
k2
D0
D1
D2
Temperature
kr1
kr2
B
1µmol.m-2.s-1
Absorbance (725nm)
Time (min)
10ºC
20ºC
25ºC
30ºC
C
5µmol.m-2.s-1
Absorbance (725nm)
Time (min)
10ºC
25ºC
30ºC
D
1µmol.m-2.s-1
Δ Absorbance
Wavelength (nm)
10ºC
20ºC
25ºC
30ºC
E
5µmol.m-2.s-1
Δ Absorbance
Wavelength (nm)
10ºC
25ºC
30ºC
F
D2
Pfr
Temperature (ºC)
G
kr1 (min-1)
Temperature (ºC)

Fig. 1

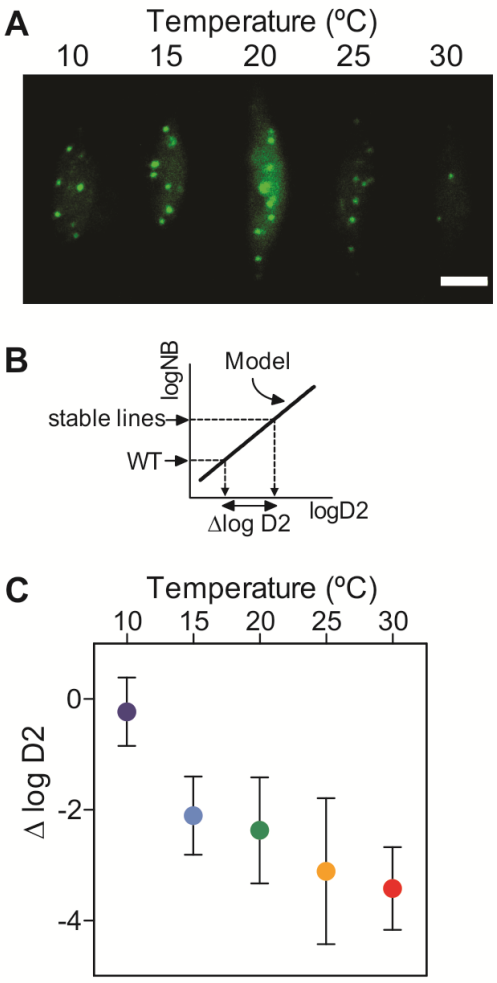
A
Temperature (ºC)
10
15
20
25
30
B
logNB
Model
stable lines
WT
ΔlogD2
logD2
C
Temperature (ºC)
10
15
20
25
30
0
-2
-4
Δ log D2

Fig. 2

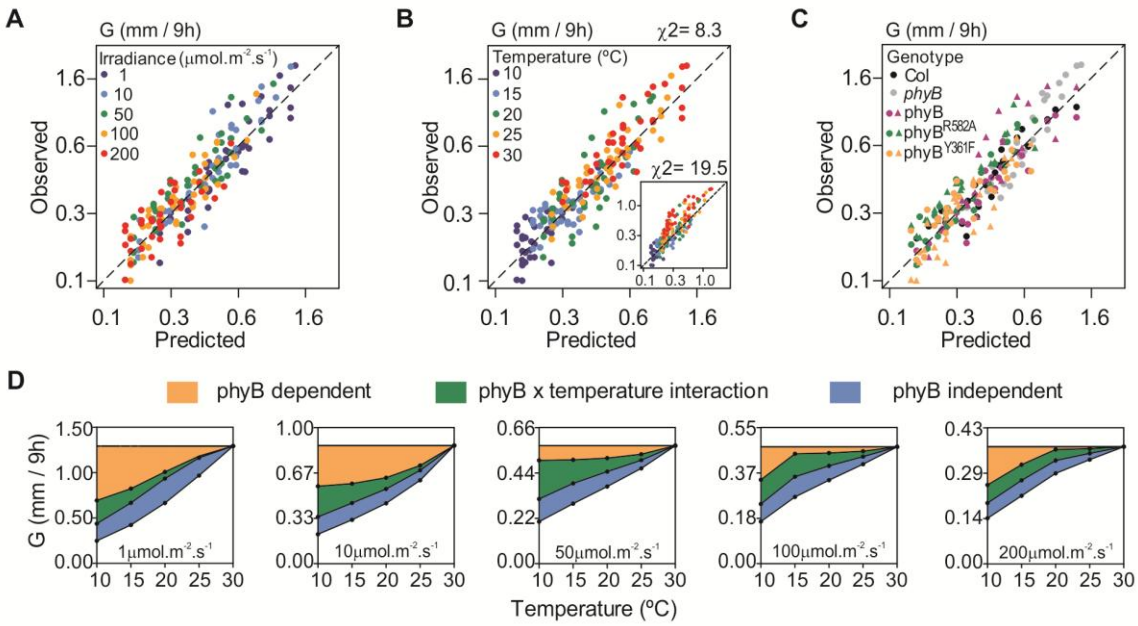
A
G (mm / 9h)
Irradiance (µmol.m-2.s-1)
1
10
50
100
200
Observed
Predicted
B
G (mm / 9h)
χ2= 8.3
Temperature (°C)
10
15
20
25
30
χ2= 19.5
C
G (mm / 9h)
Genotype
Col
phyB
phyB
phyBR582A
phyBY361F
D
phyB dependent
phyB x temperature interaction
phyB independent
G (mm / 9h)
1µmol.m-2.s-1
10µmol.m-2.s-1
50µmol.m-2.s-1
100µmol.m-2.s-1
200µmol.m-2.s-1
Temperature (°C)

Fig. 3

Supplementary Materials for

Phytochrome B integrates light and temperature signals in Arabidopsis

Martina Legris, Cornelia Klose, E. Sethe Burgie, Cecilia Costigliolo, Maximiliano Neme, Andreas Hiltbrunner, Philip A. Wigge, Eberhard Schäfer, Richard Vierstra, Jorge J. Casal

correspondence to: casal@ifeva.edu.ar

This PDF file includes:

Materials and Methods

Expression and purification of full-length *Arabidopsis thaliana* phytochrome B.

Full-length phytochrome B (phyB) with an N-terminal MGSSHHHHHHSSEN LYFQG-tag was expressed in *E. coli* BL21 (DE3) using a pBAD Myc His plasmid (Invitrogen). The pL-PΦB plasmid was also present to follow *in situ* synthesis of linear tetrapyrrole chromophore phytochromobilin (PΦB) (*15, 16*). Cultures were grown in terrific broth that included 1 mM $MgCl_2$. After cultures reached an optical density of 1 at 600 nm the temperature was set to 16º C, and 5-aminolevulinic acid was added to a final concentration of 20 μg . ml^{-1}. After one hour isopropyl β-D-1-thiogalactopyranoside was added to a final concentration of 1 mM, and after a second hour L-arabinose was added at 2 g. l^{-1}. Cultures were grown overnight and harvested by centrifugation. Cell pellets were frozen in liquid nitrogen, and stored at -80º C.

Cells were lysed in Lysis buffer, which included 10% glycerol, 500 mM NaCl, 0.05% Tween 20, 30 mM imidazole, 1 mM phenylmethanesulfonyl fluoride, 2 mM 2-mercaptoethanol, 1 tablet/liter Roche EDTA-free Complete protease inhibitor, and 20 mM HEPES-NaOH (pH 7.8). Lysates were clarified by centrifugation, and loaded onto a Ni-NTA column (Qiagen). After rinsing the column with Lysis buffer, the protein was eluted with Lysis buffer supplemented with 300 mM imidazole. The eluate was exchanged into a buffer containing 10% glycerol, 20 mM NaCl, 10 mM 2-mercaptoethanol, 1 mM ethylenediaminetetraacetate tetrasodium salt, 1 mM phenylmethanesulfonyl fluoride, 1 tablet/liter Roche EDTA-free Complete protease inhibitor, and 20 mM HEPES-NaOH (pH 7.8), and loaded onto a Q-sepharose HP column (GE). Protein was eluted using a 20-500 mM linear gradient of NaCl over 20 column volumes. Full length phyB fractions were exchanged into lysis buffer that lacked Roche protease inhibitor, and loaded onto a Ni-IMAC column (GE). Protein was eluted using a 30-150 mM imidizole gradient over 40 column volumes. The second phytochrome-containing peak was harvested, and incubated with tobacco-etch virus protease to release the N-terminal hexahistidine tag. The sample was exchanged back into lysis buffer and then passed through a Ni-NTA column that was equilibrated with the same buffer. The flow-through was collected and concentrated to an OD_{665nm} of 1. The purified protein was then frozen as droplets in liquid nitrogen. Prior to assays the protein was exchanged into the appropriate buffer using a Superose-6 column (GE). Assay buffers contained 150 mM KCl, 1 mM ethylenediaminetetraacetate tetrasodium salt, 10 mM 2-mercaptoethanol, and 50 mM HEPES-KOH pH 7.8 at the assay temperature.

In vitro spectroscopy of phyB

Spectra of dark-adapted and red-light irradiated phyB were collected using a Cary6 spectrophotometer (Agilent). Assay temperature was controlled with an Isotemp cooling/heating recirculating circulator (Fisher Scientific). Samples were irradiated from the top with a 660 nm LED. LED flux was calibrated using a Li-Cor Model LI-185B photometer. The approximate flux at the cuvette window was 1 or 5.1 μmol. m^{-2} . s^{-1}. A single cuvette was used for all measurements, and was loaded with 200 μl of phyB solution with an optical density of 0.2 at 665 nm.

Plant material.

We used seedlings of *Arabidopsis thaliana* in all the experiments. For *in vivo* spectroscopy we used seedlings over-expressing phyB in the *phyA* null mutant background (*9*). For confocal microscopy we used transgenic lines expressing phyB-YFP, phyB^{Y361F}-YFP or phyB^{R582A}-YFP (*15,16*). These lines express the wild type (WT) or mutated *PHYB* cDNA with the cDNA encoding *YFP* fused to the 3'end, under the control of the *UBQ10* promoter in the *phyB-9* background. For hypocotyl growth we used seedlings of the WT Columbia, of the *phyB-9* null mutant (*20*) and of transgenic lines expressing phyB, phyB^{Y361F} or phyB^{R582A} (two independent lines per transgene). In these lines the WT or mutated *PHYB* cDNA, are under the control of the *PHYB* promoter, in the *phyB-9* background (*15,16*). phyB^{Y361F} and phyB^{R582A} show normal photo-conversion but reduced thermal reversion (these mutants respectively retain only 2.6 and 3.5 % of the thermal reversion observed in the WT) (*15,16*).

Growth conditions.

Seeds were sown on clear plastic boxes containing 0.8 % agar-water and incubated 3-5 d at 4 °C in darkness. For *in vivo* spectroscopy, stratified seeds were transferred to full darkness at 20 °C for 4 d to obtain etiolated seedlings. For hypocotyl growth and confocal microscopy, stratified seeds were transferred to white light, 50 µmol . m^{-2} . s^{-1} provided by fluorescent tubes, photoperiod 10 h, and 20°C for 3 d. One hour after the beginning of 4th day, light-grown seedlings were transferred to the indicated combination of light and temperature (Fig. S2).

Light sources and measurements.

White light was provided by a combination of fluorescent and halogen lamps. The spectral distribution was analyzed with a USB400 (Ocean Optics) spectroradiometer (Fig. S2A). Different irradiances (1, 10, 50, 100, 200 µmol . m^{-2} . s^{-1} between 400 and 700 nm, i.e. 1.4, 14, 68, 137, 273 µmol . m^{-2} . s^{-1} between 400 and 800 nm) were obtained by means of neutral filters and by modifying the distance to the source. Red / far-red light mixtures (332/743, 220/800, 83/664, 28/618, 21/921, in µmol . m^{-2} . s^{-1} 600-700 nm/700-800 nm, Fig. S2B) were provided by 150 W incandescent R95 lamps (Philips) in combination with a yellow, orange and red acetate filter set (LEE filters 101, 105 and 106, respectively) either alone or in combination with green acetate filters (LEE filters 138, 121 or 089) or six blue acrylic filters (Paolini 2031, Buenos Aires, Argentina). Water filters were included to reduce heat and achieve the indicated temperature. Red light (330 µmol . m^{-2} . s^{-1}, Fig. S2B) was provided by a Lumi Bulb Red (Lumi Grow inc.) lamp.

In vivo Spectroscopy.

We exposed etiolated seedlings to 1 µmol . m^{-2} . s^{-1} red light (660 nm) or different intensities of white light + far-red light (740 nm) at a R:FR ratio of 1.1 for 20 min. We

transferred the seedlings to water-ice and immediately packed them into a cuvette (100–120 mg) for the *in vivo* spectroscopy analysis in a dual-wavelength ratio spectrophotometer (Ratiospect) at 4 °C. The time between the termination of red light and measurements was approximately 1 min. We measured Δ (Δ absorbance) values and used them to calculate Pfr and total phytochrome as described (*21*).

Calculation of kr1, kr2, D2, D1 and D0

The proportion of Pfr was related to D2 (proportion of Pfr-Pfr dimmers) and D1 (proportion of Pr-Pfr dimmers) and the proportion of these dimmers was related to the photochemical reactions (k1, k2) and thermal-reversion rates (kr1, kr2) by analytical equations based on the three stage phytochrome model (*11*). We calculated kr1 following equation (1):

$$kr1 = \frac{\left(2k1^2/_{Pfr}\right) + \left(k1\,[2k2 + 2\,kr2]/_{Pfr}\right) - 2k1^2 - 2k1\,(2k2 + 2kr2)}{(2k2 + 2kr2)} - k2 \qquad (1)$$

The rate of photochemical reactions was calculated by using data published by Kelly and Lagarias (*22*). The kr2 values were calculated from experiments were the seedlings were given a saturating red-light pulse followed by darkness (*19*). In seedlings exposed to a red light pulse followed by darkness, the D1 pool is rapidly depleted and therefore the limiting step for Pfr and D2 decay is controlled by kr2. The rate of decay observed in darkness corresponds to 2 kr2, because after one of the Pfr molecules of D2 reverts to Pr, the newly formed D1 rapidly reverts to D0. The rate of decay in darkness of the phytochrome present in etiolated squash seedlings (predominantly phyA) (*23*) and of phyB (*19*) is enhanced by warm temperatures. Under illumination, kr1 becomes much more important than kr2 because light reactions refresh the D1 pool. For this reason the temperature dependence of kr2 observed in darkness is not expected to have a strong impact on Pfr levels under moderate light levels.

Confocal microscopy.

To obtain confocal fluorescence images we used a LSM5 Pascal laser-scanning microscope (Zeiss) with a water immersion objective lens (C-Apochromat 40x / 1,2; Zeiss). For phyB-YFP fusion protein visualization, probes were excited with an argon laser (wavelength 488 nm), and fluorescence was detected using a BP 505-530 filter. Images were taken from the epidermis and the first sub-epidermal layers of the hypocotyl.

Image analysis.

For the analysis of phyB nuclear bodies we designed an algorithm in MatlabTM Software (R2008a).The processing algorithm contains two pieces of code: a main script, designed to collect the information from the image files present in a specified folder, and a processing function, which is called from the main script for each image in that folder. Once the processing function has been called for every image, the main script exports the information obtained from each function call into an excel file. The information obtained from each image includes the

number of granules of each size class and the mean fluorescence intensity in the area where granules are detected. The detection of granules is implemented by using a bi-dimensional correlation of the original image with three different granules used as kernels, one at the time. When the latter correlation is above a given threshold, it is assumed that a granule has been detected and its presence is properly registered in a binary mask. This binary mask is analyzed by classifying those "binarized granules" by their area into five categories arbitrary defined and also to compute the mean intensity of the image in the area where granules were detected. The diameter of 1 pixel is 0.06 μm.

We calculated the average size of the phyB nuclear bodies as described by equation (2):

$$NB = \frac{\sum_{i=0}^{c} N_c \times S_c}{\sum_{i=0}^{c} N_c} \quad (2)$$

Where *NB* is the average size of phyB nuclear bodies, *c* indicates the size class, N_c the number of nuclear bodies for class *c* and S_c the lowest limit size of class *c*.

Modeling the response of phyB nuclear bodies to D2 and temperature in the phyB^{Y361F}-YFP and phyB^{R582A}-YFP lines

Equation (3) represents the relationship between the average size of phyB nuclear bodies, phyB status (D2) and temperature conditions in the phyBY^{361F}-YFP and phyB^{R582A}-YFP lines:

$$\log NB = l + m \cdot \log D2 + n \cdot T + p \cdot T^2 \quad (3)$$

Where *T* is temperature. We fitted the equation by using the multiple regression analysis tools of Infostat (www.infostat.com.ar) (Fig. S6).

Calculating the apparent D2 in phyB-YFP.

After observing that increasing temperatures reduce phyB Pfr by *in vitro* and *in vivo* in spectroscopy (Fig. 1) we decided to evaluate the effects of temperature on phyB in light-grown seedlings (similar to those used for the analysis of the physiological output), which are not suitable for spectroscopy due to the presence of chlorophyll. For this purpose, we used the model describing the relationship between the average size of phyB nuclear bodies and D2 in the phyB^{Y361F}-YFP and phyB^{R582A}-YFP lines (Fig. S6). We used the average size of the nuclear bodies in phyB-YFP as input to the model to estimate the D2 of WT phyB-YFP under the different light and temperature conditions (Fig. 2B). Therefore, for each light-temperature condition we had the estimated D2 value of the WT, which depends on the balance of photochemical (k1, k2) and thermal (kr1, kr2) reactions, and the D2 value of the stabilized mutants, which depends largely on the balance of photochemical reactions (k1, k2). The difference between these two log-transformed D2 values provides an estimate of the impact of thermal reactions, because the latter are negligible in the phyB^{Y361F}-YFP and phyB^{R582A}-YFP lines. This Δ log D2 value (averaged for the different light conditions) plotted against temperature offers an estimate of the impact of temperature on phyB status that is independent of the spectroscopic analysis (Fig. 2C).

The aim of this approach is to quantify temperature effects on phyB status D2 by comparing nuclear body formation in the WT and stabilized lines, where temperature effects on D2 are negligible due to the severely deficient thermal reversion. However, temperature has additional effects on nuclear body formation that likely reflect changes in the balance of phyB aggregation / dissociation rates once a given D2 is established by light and (in the case of the WT) temperature conditions. For instance, in the phyB^{Y361F}-YFP and phyB^{R582A}-YFP lines, temperature has a dual effect on average nuclear body size at a given D2 (Fig. S6). In the phyB-YFP line, temperature has a dual effect (Fig. 2A, Fig S5) and the positive effect is not mediated by changes in D2 (because higher temperatures reduce D2, Fig. 1, and D2 increases nuclear body formation(*11*)). To estimate the D2-independent effect of temperature in the WT we fitted the ascending portion of the response to temperature to a straight line (for instance, between 10 and 20°C in Fig. S5) for each light condition and averaged the slope for all light conditions (0.011 ±0.002 μm . °C^{-1}). In order to use average nuclear body size of the WT to estimate its D2 values as affected by temperature, the D2-independent effects of temperature have to be corrected. For this purpose, we used the model relating D2 to average nuclear body size in the phyB^{Y361F}-YFP and phyB^{R582A}-YFP lines at 10°C as a calibration curve. In the WT, we normalized the D2-independent effect on nuclear body size to 10°C by multiplying the difference between 10°C and the relevant temperature by the D2-independent temperature effect (0.011 ±0.002 μm . °C^{-1}). Since the ascending branch of the nuclear body size response to temperature is actually the balance between D2-independent and D2-dependent effects, the coefficient used for the correction of nuclear body size in the WT would be slightly underestimated. The consequence of the latter is that the impact of temperature on D2 reported in Fig. 2C is also underestimated, which does not affect the conclusions of this paper.

Growth measurements.

We photographed the seedlings with a digital camera 1 h and 10 h after the beginning of the 4th day and measured hypocotyl length using image processing software (*28*). We present length increments for the 9-h period. Therefore, light and temperature treatments were applied simultaneously and growth measurements covered exactly the duration of these treatments (Fig. S2).

Modeling the relationship between stem growth and the factors that inhibit growth.

Stem (hypocotyl) growth depends on the integration of different inputs, and changing the level of one of them typically affects the impact of the other. Reduced phytochrome activity could render hypocotyl growth close to the upper limit, impairing the ability of warm temperatures to further promote growth. Increased phytochrome activity could place the inputs inhibiting growth in the saturation zone also impairing the temperature response. Therefore, to investigate whether temperature effects are mediated by phyB perception we quantitatively modeled growth. If phyB mediates effects of temperature, changing D2 by light, temperature, or by stabilizing mutations should have the same effect.

Following the general structure of previous growth models (*18*, *25*), we modeled growth as a function of its maximum attainable rate, divided by the sum of terms representing the factors that inhibit growth. Equation (4) represents the relationship between growth and the inhibitory actions of phyB, low temperatures and other photoreceptors:

$$G = \frac{G_0}{1+K\cdot D2+a\cdot([{}^1/_T]-[{}^1/_{30°C}])+b\cdot I+c\cdot D2\cdot([{}^1/_T]-[{}^1/_{30°C}])} \quad (4)$$

Where *G* indicates growth, G_0, maximal growth, *I*, irradiance and *T*, temperature. Maximal growth rate was 1.9 mm / 9 h, achieved by the *phyB* mutant at 30°C, 10 or 1 µmol . m^{-2} . s^{-1}. Under these conditions there is no inhibition by phyB (*phyB* mutant), low temperatures (temperatures higher than 30°C do not promote growth rate) or other photoreceptors (no difference between 1 and 10 µmol . m^{-2} . s^{-1}).

To parameterize the model, we first fitted Go/G (higher values indicate stronger inhibition) against each component of the growth model separately, using linear regression and specific subsets of data that minimize the contribution of the other factors. We then tested the significance of all possible interactions among these terms.

Calculation of the contribution of phyB-dependent and phyB-independent terms to the response of growth to temperature.

For the different irradiances and temperatures, we first estimated growth keeping D2 at the values corresponding to 30°C and *T*= 30°C for the temperature and D2-temperature interaction terms (which become null) (Fig. S11). This provided a horizontal baseline where none of the three temperature-dependent terms is varied (Fig. 3D). We then estimated growth keeping *T*= 30°C for the temperature and D2-temperature interaction terms; i.e., the only effect of temperature is to modify D2. Subsequently, we estimated growth keeping *T*= 30°C only for the temperature term; i.e. temperature modifies the D2 and interaction terms. Finally, we estimated growth without fixing the values of *T*; i.e. temperature modifies the three terms.

References

20. J. W. Reed, P. Nagpal, D. S. Poole, M. Furuya, J. Chory, *Plant Cell*. **5**, 147–157 (1993).
21. L. Hennig, C. Büche, K. Eichenberg, E. Schäfer, *Plant Physiol.* **121**, 571–577 (1999).
22. J. M. Kelly, J. C. Lagarias, *Biochem.* **24**, 6003–6010. (1985).
23. E. Schäfer, W. Schmidt, *Planta*. **116**, 257–266 (1974).
24. R. Sellaro, U. Hoecker, M. Yanovsky, J. Chory, J. J. Casal, *Curr. Biol.* **19**, 1216–1220 (2009).
25. J. Rausenberger *et al.*, *PLoS One*. **5** (2010).
26. H. Johansson *et al.*, *Nat. Commun.* **5**, 4848 (2014).

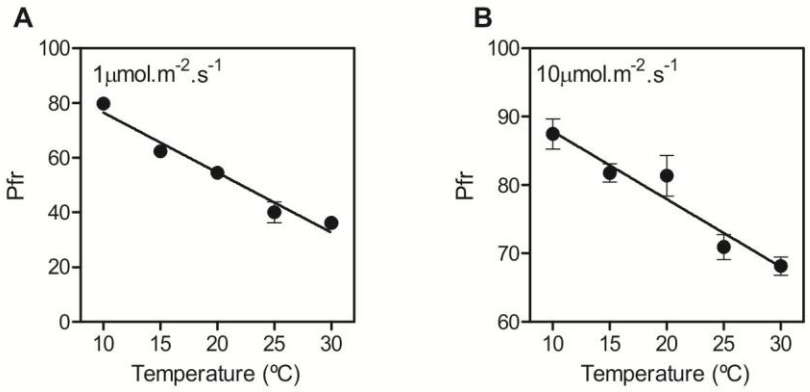

Fig. S1. Warm temperatures reduce the levels of Pfr *in vivo*

Percentage of Pfr measured in *phyA* mutant seedlings overexpressing phyB (*9*) exposed to 1or 10 μmol . m^{-2} . s^{-1} white light and the indicated temperatures. Means ±SE of 3 biological replicates. The effect of temperature is significant at P = 0.0031 (A) and P = 0.0074 (B).

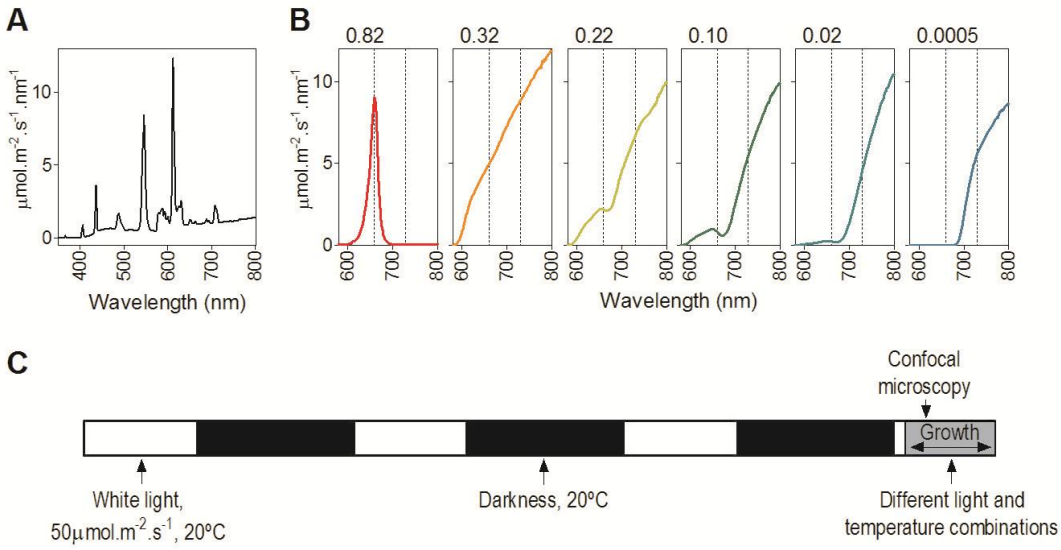

Fig. S2.Spectral photon distribution of the light sources and experimental protocol.

(**A**) White light. (**B**) Red light, far-red light and red plus far-red light mixtures (D2 values are indicated above each figure). (**C**) Experimental protocol.

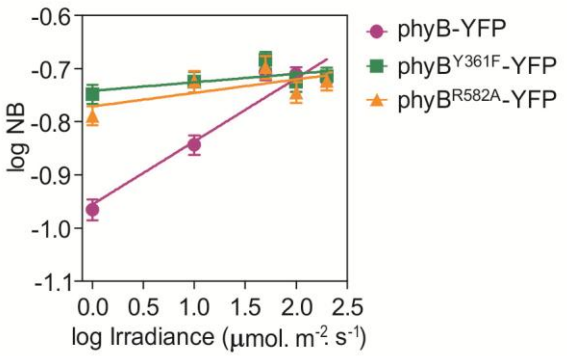

Fig. S3. Reduced response of phyB average nuclear body size (NB) to changes in white-light irradiance in the phyB^{Y361F}-YFP and phyB^{R582A}-YFP compared to the phyB-YFP lines.

Arabidopsis seedlings were grown as described in Fig. S2 and exposed to the indicated irradiances (data from Table S1, average of all temperatures). The response to irradiance depends on the competition between light reactions (k1, k2) and thermal reversion (kr1, kr2). The phyB^{Y361F}-YFP and phyB^{R582A}-YFP lines have severely reduced thermal reversion and therefore, deficient responses to irradiance. The slope of the WT phyB-YFP is significantly stronger than that of the stabilized mutants (pooled data for phyB^{Y361F}-YFP and phyB^{R582A}-YFP) at $P < 0.0001$. When the regression analysis is conducted separately for each genotype, the slope of the WT phyB-YFP is significant at $P<0.0001$ and the slopes of phyB^{Y361F}-YFP and phyB^{R582A}-YFP are not significant ($P = 0.20$ and $P = 0.10$, respectively).

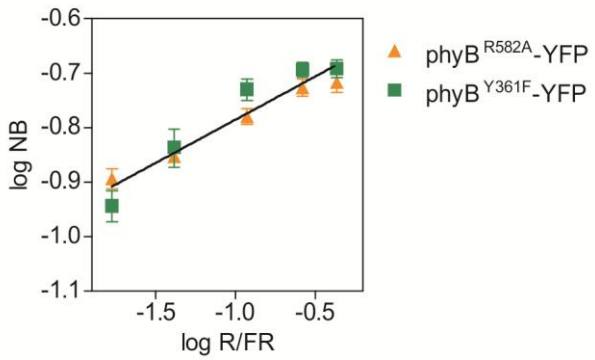

Fig. S4. Response of phyB average nuclear body size (NB) in phyB^{Y361F}-YFP and phyB^{R582A}-YFP to changes in red / far-red ratio.

Arabidopsis seedlings were grown as described in Fig. S2 and exposed to the indicated red / far-red ratios (R/FR) (data from Table S2, average of all temperatures). Although phyB^{Y361F}-YFP and phyB^{R582A}-YFP show no significant response to irradiance (Fig. S3) due to their severely reduced thermal reversion, they retain responses to the red / far-red ratio, which modifies D2 by changing the balance of photo-transformation reactions (k1 and k2). The slope is significant at P = 0.0019 (pooled data for phyB^{Y361F}-YFP and phyB^{R582A}-YFP), P = 0.0010 (phyB^{Y361F}-YFP) and P = 0.0013 (phyB^{R582A}-YFP).

.

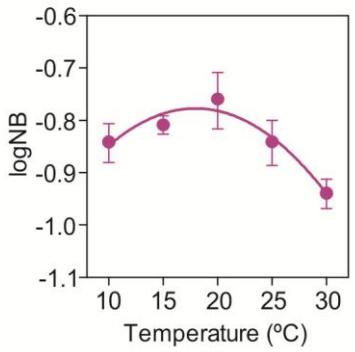

Fig. S5. Quadratic effect of temperature on the average size of phyB nuclear bodies (NB) in the WT.

Arabidopsis seedlings were grown as described in Fig. S2 and exposed to the indicated temperatures (data from Table S1, 10 µmol . m^{-2} . s^{-1}). Representative pictures are shown in Fig. 2A. The linear and quadratic terms are significant at $P < 0.05$.

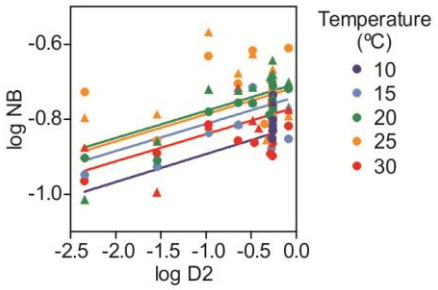

Fig. S6. Relationship between of phyB average nuclear body size (NB) and D2 and temperature in phyB^{Y361F}-YFP and phyB^{R582A}-YFP.

Arabidopsis seedlings were grown as described in Fig S2 and exposed to different irradiances and red / far-red ratios in combination with different temperatures applied only during the different light treatments (data from Tables S1 and S2). Data are fitted to equation (3) $\log NB = l + m \cdot \log D2 + n \cdot T + p \cdot T^2$, where *l*= -1.11 ±0.07 log µm; *m* = 0.07 ±0.01 log µm; *n*= 0.04 ±0.01 log µm/°C; and *p*= -0.0009 ±0.0002 log µm/°C^2. *l*, *m*, *n*, and *p* are significant at P <0.0001.

● = phyB^{R582A}-YFP; ▲ = phyB^{Y361F}-YFP

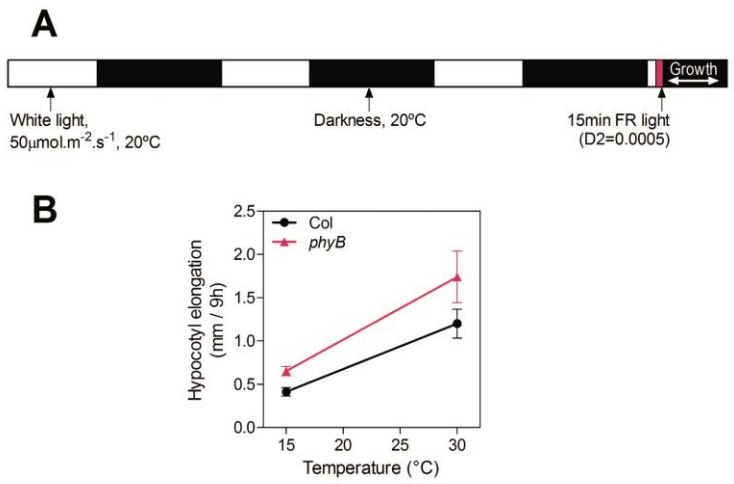

Fig. S7. Hypocotyl growth response to temperature in the absence of phyB and other photoreceptor activity.

(**A**) Protocol. Seedlings of the WT Columbia (Col) and of the *phyB* mutant were given a far-red light pulse (to minimize phytochrome activity) and transferred to darkness (to minimize other photoreceptor activity) 1 h after the beginning of day 4. Hypocotyl growth was measured during the subsequent 9 h. (**B**) Rate of hypocotyl growth. Data are means and SE of 9 replicate boxes of seedlings. The effect of temperature is significant at $P < 0.001$ for Col and *phyB* mutant seedlings.

Since temperature affects growth in the absence of photoreceptor activity we conclude that not all the effect of temperature is mediated by changes in photoreceptor activity.

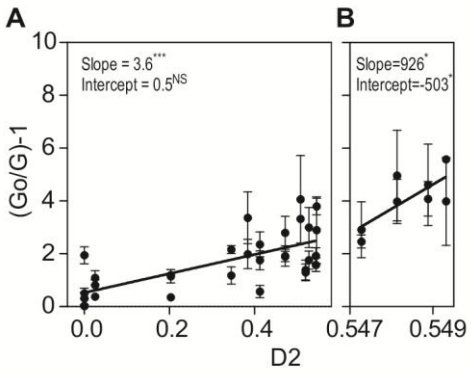

Fig. S8. Contribution of phyB to the inhibition of hypocotyl growth.

The inverse of growth is plotted against D2. Data correspond to seedlings of the Columbia WT, of transgenic lines expressing phyB, phyB^{Y361F} or phyB^{R582A} in the *phyB* null mutant background, and of the *phyB* null mutant background (D2= 0) grown at 30 °C (no low temperature growth inhibition) from table S3. (**A**) Range of lower D2. (**B**) Range of higher D2. Mean ±SE from table S3; ***, P <0.001; *, P<0.05, NS, not significant. A single K has been used to account for phyB-mediated growth inhibition under continuous red light in etiolated seedlings (*11*) but white-light grown seedlings typically show a sharp response to reductions in phyB activity below sunlight values (*18*), which provides sensitivity to the signals of neighboring vegetation and triggers shade avoidance.

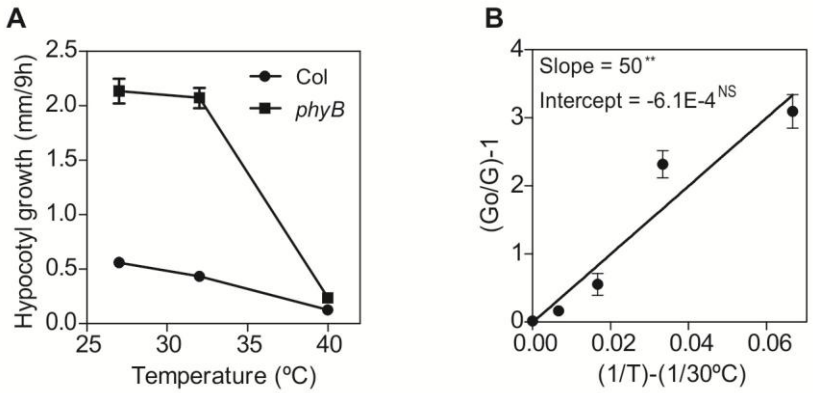

Fig. S9. Contribution of low temperatures to the inhibition of growth independently of active phyB and other photoreceptors.

(**A**) Hypocotyl growth rate decreases when the seedlings are exposed to temperatures higher than 30°C. At 30°C growth is maximal and there is no inhibition by low temperatures. Data correspond to the WT and to the *phyB* mutant. Means ±SE of 5 replicate boxes. Similar results were obtained in 3 independent experiments. (**B**) The inverse of growth plotted against the inverse of temperature minus a threshold to indicate no inhibition at 30°C. Data correspond to the *phyB* mutant (no phyB-mediated inhibition) exposed to 1 µmol . m^{-2} . s^{-1} (at 1 and 10 µmol . m^{-2} . s^{-1} and 30°C, growth is maximal, indicating that other photoreceptors do not make a strong contribution). Means ±SE from table S3. **, P <0.01; NS, not significant.

In Arabidopsis seedlings grown under continuous red light from seed germination to final hypocotyl length at 28°C, increasing irradiance beyond intermediate values actually promotes hypocotyl growth in contrast to increasing irradiance in the lower range. At 17°C increasing irradiances inhibit growth in the whole range (*26*). This phenomenon is called “photo-thermal switch” (*26*). Although we can reproduce the photo-thermal switch under the conditions described in the literature, we found no evidence for light promotion of hypocotyl growth under the conditions used here. There are several differences in experimental protocols that could account for the diverse output, including the analysis of final hypocotyl length vs. length increment over a shorter time, the use of continuous light vs. light / dark cycles, and the use red light vs. white light (which also activates cryptochromes).

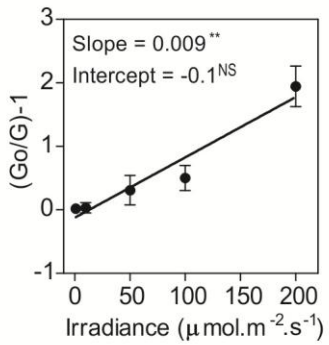

Fig. S10. Contribution of the activity of photoreceptors other than phyB to the inhibition of hypocotyl growth.

Inverse of growth plotted against irradiance. Data correspond to the *phyB* mutant (no phyB-mediated inhibition) at 30 °C (no low-temperature growth inhibition). Means ±SE from table S3. **, P <0.01; NS, not significant.

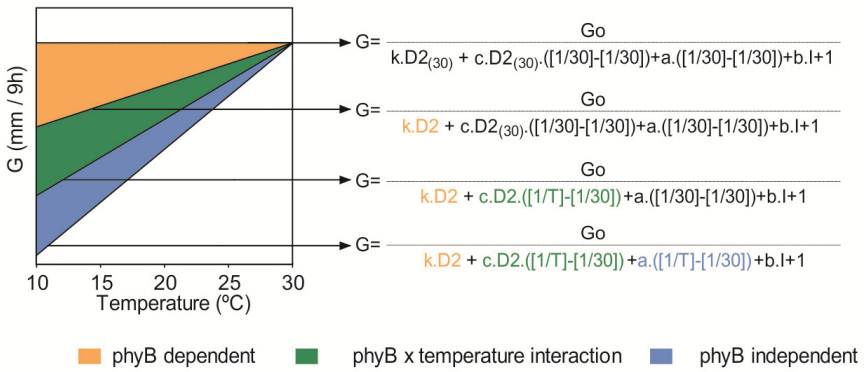

Fig. S11 Calculation of the contribution to growth inhibition of each of the temperature-dependent terms of the growth model.

Equation (4) was used to calculate the effect of different temperature-dependent terms on growth. The upper (horizontal) line corresponds to the case where all the temperature-dependent terms were set to the values corresponding to 30ºC (i.e., D2= $D2_{(30)}$ and T=30ºC). In each one of the downstream lines we sequentially replaced D2 and/or T by the value corresponding to the temperature indicated in abscissas. The area between lines describes the contribution of each term.

Table S1. phyB nuclear bodies respond to light and temperature.

Number of phyB nuclear bodies of five different size classes as affected by 25 combinations of light and temperature in transgenic lines expressing phyB-YFP, phyB^{Y361F}-YFP or phyB^{R582A}-YFP.

Genotype	Temperature (ºC)	Irradiance ($\mu mol.m^{-2}.s^{-1}$)	Number per size class (size in μm^2)										NB (μm^2)		N (nuclei)
			>0.32		0.32-0.24		0.24-0.16		0.16-0.08		0.08-0.03				
			Mean	SE	Mean	SE	Mean	SE	Mean	SE	Mean	SE	Mean	SE	
phyB	10	1	0.13	0.06	0.38	0.14	3.09	0.48	3.84	0.67	3.47	0.73	0.10	0.01	32
phyB	10	10	0.88	0.28	1.04	0.29	3.63	0.61	3.21	0.56	3.67	0.79	0.13	0.01	24
phyB	10	50	0.82	0.23	1.50	0.37	2.82	0.50	1.09	0.31	0.82	0.27	0.16	0.01	22
phyB	10	100	0.92	0.21	1.17	0.24	2.50	0.40	1.46	0.45	2.04	0.80	0.17	0.01	24
phyB	10	200	0.67	0.17	1.08	0.22	4.29	0.56	1.00	0.23	1.25	0.31	0.16	0.01	24
phyB	15	1	0.00	0.00	0.17	0.11	3.33	0.87	4.67	0.98	4.08	1.52	0.08	0.01	12
phyB	15	10	0.08	0.08	0.83	0.32	5.83	0.89	2.25	0.45	0.92	0.42	0.14	0.01	12
phyB	15	50	0.30	0.15	0.80	0.36	1.90	0.38	1.10	0.41	0.90	0.48	0.15	0.02	10
phyB	15	100	0.50	0.23	1.42	0.38	3.50	0.79	1.50	0.62	1.00	0.37	0.16	0.01	12
phyB	15	200	0.50	0.19	1.75	0.41	4.75	0.98	1.08	0.29	1.08	0.38	0.16	0.01	12
phyB	20	1	0.25	0.18	0.75	0.37	2.75	0.86	2.08	0.75	1.67	0.50	0.10	0.02	12
phyB	20	10	0.50	0.26	1.58	0.60	3.75	0.73	2.75	0.72	1.00	0.21	0.15	0.02	12
phyB	20	50	1.50	0.56	1.60	0.48	1.70	0.26	1.10	0.23	0.40	0.22	0.19	0.01	10
phyB	20	100	0.92	0.36	1.58	0.43	2.92	0.71	0.75	0.25	0.58	0.23	0.18	0.01	12
phyB	20	200	0.67	0.36	1.00	0.25	2.50	0.40	0.58	0.29	0.83	0.30	0.16	0.01	12
phyB	25	1	0.00	0.00	0.00	0.00	4.17	1.03	6.42	1.37	2.50	0.58	0.10	0.01	12
phyB	25	10	0.17	0.11	0.58	0.26	4.67	0.97	1.67	0.43	0.67	0.26	0.13	0.01	12
phyB	25	50	1.40	0.52	1.20	0.33	3.30	0.47	1.10	0.41	0.80	0.29	0.18	0.01	10
phyB	25	100	0.92	0.36	1.67	0.38	2.42	0.36	0.67	0.26	1.17	0.56	0.18	0.01	12
phyB	25	200	0.58	0.19	2.08	0.23	3.83	0.77	0.92	0.29	0.50	0.19	0.18	0.01	12
phyB	30	1	0.00	0.00	0.17	0.09	2.21	0.44	2.07	0.42	3.28	0.68	0.08	0.01	29
phyB	30	10	0.10	0.10	0.35	0.13	2.80	0.50	1.80	0.44	2.30	0.55	0.10	0.01	20
phyB	30	50	0.85	0.25	1.50	0.33	2.50	0.44	0.40	0.13	0.60	0.18	0.18	0.01	20
phyB	30	100	0.85	0.28	1.65	0.34	1.50	0.35	0.50	0.18	1.80	0.68	0.17	0.01	20
phyB	30	200	0.95	0.26	1.30	0.30	1.90	0.35	0.30	0.13	1.15	0.43	0.17	0.01	20
phyB^{R582A}	10	1	1.06	0.26	0.72	0.18	3.06	0.65	2.88	0.60	3.16	0.58	0.14	0.01	32
phyB^{R582A}	10	10	1.38	0.23	0.75	0.23	2.33	0.64	1.58	0.57	2.58	0.88	0.18	0.02	24
phyB^{R582A}	10	50	0.77	0.21	0.77	0.24	1.41	0.36	2.18	0.62	1.23	0.32	0.16	0.02	22
phyB^{R582A}	10	100	0.75	0.20	0.88	0.16	2.88	0.58	2.29	0.65	3.17	0.81	0.15	0.01	24
phyB^{R582A}	10	200	1.54	0.33	1.33	0.23	2.71	0.54	1.29	0.34	1.25	0.39	0.18	0.01	24
phyB^{R582A}	15	1	0.50	0.23	0.75	0.28	3.75	1.14	3.00	1.13	2.58	1.14	0.13	0.01	12
phyB^{R582A}	15	10	0.58	0.31	1.08	0.31	2.50	0.66	1.17	0.51	1.17	0.39	0.15	0.02	12
phyB^{R582A}	15	50	0.60	0.34	1.60	0.45	4.40	1.37	2.40	1.24	1.60	0.65	0.18	0.02	10
phyB^{R582A}	15	100	0.67	0.22	1.17	0.34	1.50	0.68	1.33	0.45	0.75	0.35	0.15	0.02	12
phyB^{R582A}	15	200	0.58	0.34	1.17	0.34	1.83	0.65	1.58	0.54	2.00	0.65	0.16	0.02	12

phyB^{R582A}	20	1	1.00	0.43	0.50	0.29	4.67	1.28	1.67	0.62	2.67	0.79	0.16	0.02	12
phyB^{R582A}	20	10	1.50	0.40	0.67	0.26	1.50	0.69	1.42	0.72	1.17	0.46	0.20	0.02	12
phyB^{R582A}	20	50	1.80	0.49	0.60	0.22	1.50	0.67	2.30	0.98	1.70	0.63	0.20	0.03	10
phyB^{R582A}	20	100	1.33	0.40	0.92	0.23	2.83	1.28	0.92	0.40	0.50	0.19	0.19	0.02	12
phyB^{R582A}	20	200	0.58	0.34	1.50	0.36	1.33	0.45	0.58	0.23	1.00	0.41	0.17	0.02	12
phyB^{R582A}	25	1	0.25	0.18	1.08	0.29	3.92	0.43	2.08	1.04	0.92	0.54	0.15	0.01	12
phyB^{R582A}	25	10	0.38	0.18	0.92	0.21	3.62	0.80	1.00	0.47	0.62	0.38	0.17	0.01	13
phyB^{R582A}	25	50	0.70	0.30	1.30	0.37	2.00	0.49	0.70	0.42	0.90	0.50	0.19	0.02	10
phyB^{R582A}	25	100	0.58	0.23	1.33	0.28	2.67	0.73	0.58	0.26	0.25	0.13	0.19	0.01	12
phyB^{R582A}	25	200	0.67	0.28	1.42	0.40	1.25	0.49	0.83	0.66	0.83	0.39	0.19	0.02	12
phyB^{R582A}	30	1	0.13	0.08	1.07	0.24	2.47	0.24	1.33	0.43	1.63	0.41	0.14	0.01	30
phyB^{R582A}	30	10	0.55	0.29	1.40	0.33	2.30	0.39	2.10	0.66	3.10	0.70	0.13	0.01	20
phyB^{R582A}	30	50	0.45	0.22	1.35	0.21	1.90	0.48	0.90	0.31	0.90	0.28	0.18	0.01	20
phyB^{R582A}	30	100	0.29	0.16	1.29	0.31	1.81	0.33	1.10	0.50	3.62	1.27	0.13	0.01	21
phyB^{R582A}	30	200	0.25	0.12	1.35	0.37	2.05	0.33	0.90	0.33	2.45	0.82	0.14	0.01	20
phyB^{Y361F}	10	1	0.63	0.18	0.78	0.20	3.28	0.70	2.25	0.44	2.38	0.64	0.16	0.01	32
phyB^{Y361F}	10	10	0.58	0.25	0.75	0.19	3.50	0.52	2.00	0.56	2.25	0.69	0.15	0.01	24
phyB^{Y361F}	10	50	0.82	0.24	0.95	0.28	3.05	0.54	1.23	0.44	0.73	0.24	0.18	0.01	22
phyB^{Y361F}	10	100	0.67	0.21	1.00	0.28	3.38	0.66	1.63	0.39	2.25	0.63	0.15	0.01	24
phyB^{Y361F}	10	200	0.46	0.26	0.75	0.23	2.25	0.40	0.83	0.23	0.71	0.22	0.16	0.01	24
phyB^{Y361F}	15	1	0.25	0.18	1.17	0.44	2.83	0.61	1.67	0.67	0.75	0.28	0.14	0.01	12
phyB^{Y361F}	15	10	0.33	0.22	0.92	0.31	4.92	1.27	0.75	0.28	0.75	0.28	0.18	0.02	12
phyB^{Y361F}	15	50	0.30	0.15	1.60	0.50	4.30	1.09	1.20	0.39	0.60	0.27	0.17	0.01	10
phyB^{Y361F}	15	100	0.50	0.26	1.00	0.28	4.25	0.69	0.75	0.30	0.42	0.15	0.17	0.01	12
phyB^{Y361F}	15	200	0.42	0.29	0.92	0.26	2.75	0.55	0.42	0.19	0.25	0.13	0.18	0.02	12
phyB^{Y361F}	20	1	0.92	0.36	0.67	0.26	1.92	0.57	0.25	0.18	0.58	0.42	0.21	0.02	12
phyB^{Y361F}	20	10	1.64	0.49	0.73	0.27	1.00	0.50	1.00	0.43	0.18	0.12	0.23	0.02	11
phyB^{Y361F}	20	50	1.00	0.30	0.70	0.21	1.80	0.57	0.40	0.16	0.10	0.10	0.21	0.02	10
phyB^{Y361F}	20	100	0.50	0.29	1.17	0.30	1.83	0.47	0.58	0.34	0.58	0.23	0.18	0.02	12
phyB^{Y361F}	20	200	0.67	0.31	1.17	0.44	2.00	0.44	0.33	0.26	0.42	0.29	0.18	0.01	12
phyB^{Y361F}	25	1	0.00	0.00	0.67	0.26	2.58	0.47	0.75	0.25	0.33	0.14	0.14	0.01	12
phyB^{Y361F}	25	10	0.38	0.21	1.08	0.29	2.23	0.52	1.31	0.98	3.00	2.42	0.17	0.02	13
phyB^{Y361F}	25	50	0.50	0.27	0.90	0.35	2.50	0.72	0.20	0.13	0.10	0.10	0.19	0.01	10
phyB^{Y361F}	25	100	0.67	0.31	1.58	0.36	1.67	0.53	0.25	0.13	0.50	0.26	0.20	0.01	12
phyB^{Y361F}	25	200	0.83	0.27	1.08	0.34	2.25	0.57	0.17	0.11	0.17	0.11	0.22	0.02	12
phyB^{Y361F}	30	1	0.19	0.12	0.62	0.19	2.50	0.24	0.38	0.15	1.23	0.51	0.15	0.01	26
phyB^{Y361F}	30	10	0.50	0.24	1.05	0.32	2.00	0.36	0.60	0.17	1.80	0.69	0.15	0.01	20
phyB^{Y361F}	30	50	0.55	0.29	1.05	0.27	1.85	0.33	0.40	0.18	0.35	0.13	0.18	0.01	20
phyB^{Y361F}	30	100	0.35	0.22	0.85	0.25	1.80	0.26	0.40	0.18	2.70	1.18	0.15	0.01	20
phyB^{Y361F}	30	200	0.40	0.17	0.80	0.22	2.10	0.40	0.65	0.20	1.80	0.68	0.14	0.01	20

Table S2. phyB nuclear bodies respond to red/far-red light ratio.

Number of phyB nuclear bodies of five different size classes as affected by five different red / far-red ratios of the light and temperatures ranging from 15 to 30ºC, in transgenic lines expressing phyB-YFP, phyB^{Y361F}-YFP or phyB^{R582A}-YFP.

Genotype	R/FR	Temperature (ºC)	Number per size class										NB (µm^2)		N (nuclei)
			>0.32		0.32-0.24		0.24-0.16		0.16-0.08		0.08-0.03				
			mean	SE	mean	SE	mean	SE	mean	SE	mean	SE	mean	SE	
phyB	Red	15	0.25	0.1	1	0.4	5.167	0.9	1.75	0.7	0.75	0.3	0.169	0.01	12
phyB	0.77	15	0.083	0.1	0.583	0.3	2.75	0.7	1.583	0.5	0.75	0.2	0.131	0.015	12
phyB	0.45	15	0	0	0.167	0.1	3.5	1	2.75	0.8	2.167	0.7	0.109	0.012	12
phyB	0.2	15	0	0	0	0	1.917	0.9	3.667	1.1	2.5	0.5	0.077	0.01	12
phyB	0.07	15	0	0	0	0	0.167	0.1	1.667	0.7	0.5	0.2	0.034	0.012	12
phyB	0.001	15	0	0	0	0	0.25	0.3	1.833	1	1.833	0.7	0.028	0.009	12
pHYB^{R582A}	Red	15	0	0	0.636	0.3	4.273	0.8	1.091	0.5	0.545	0.3	0.146	0.018	11
pHYB^{R582A}	0.77	15	0	0	0.417	0.2	5.25	0.9	0.917	0.2	0.083	0.1	0.171	0.005	12
pHYB^{R582A}	0.45	15	0	0	0.167	0.2	4.583	0.9	1.167	0.3	0.583	0.2	0.156	0.008	12
pHYB^{R582A}	0.2	15	0	0	0.417	0.3	4.167	0.8	2.083	0.6	0.833	0.4	0.146	0.008	12
pHYB^{R582A}	0.07	15	0	0	0.083	0.1	2.917	0.7	3.75	0.5	1.333	0.3	0.112	0.008	12
pHYB^{R582A}	0.001	15	0	0	0.167	0.2	3.167	1	2.583	0.8	1.583	0.5	0.083	0.019	12
phyB^{Y361F}	Red	15	0.333	0.2	1	0.4	3.5	1	1.667	0.4	1.667	0.8	0.167	0.017	12
phyB^{Y361F}	0.77	15	0.083	0.1	0.5	0.3	6.083	0.9	2.5	0.6	1.167	0.4	0.147	0.007	12
phyB^{Y361F}	0.45	15	0	0	0.583	0.4	7.417	1.6	2.167	0.5	1.333	0.3	0.149	0.006	12
phyB^{Y361F}	0.2	15	0	0	0.333	0.2	7.25	1.4	3.75	0.8	1.25	0.5	0.14	0.011	12
phyB^{Y361F}	0.07	15	0.167	0.1	0.25	0.1	4.583	1.2	4.917	0.7	2	0.4	0.112	0.007	12
phyB^{Y361F}	0.001	15	0	0	0	0	5.083	1.2	5.833	1.3	3.333	0.8	0.105	0.007	12
phyB	Red	20	0.667	0.1	1.588	0.1	2.314	0.2	0.353	0.1	0.471	0.1	0.217	0.007	51
phyB	0.77	20	0.5	0.1	1.192	0.2	3.75	0.3	1.115	0.2	0.615	0.1	0.182	0.006	52
phyB	0.45	20	0.196	0.1	1.059	0.1	3.314	0.3	1.157	0.2	0.765	0.2	0.167	0.008	51
phyB	0.2	20	0.058	0.1	0.077	0	1.385	0.2	2.192	0.3	1.365	0.2	0.083	0.006	52
phyB	0.07	20	0	0	0	0	0.462	0.1	1.654	0.3	1.327	0.2	0.051	0.006	52
phyB	0.001	20	0.019	0	0	0	0.096	0	1.077	0.2	2.096	0.4	0.038	0.004	52
pHYB^{R582A}	Red	20	0.731	0.2	1.558	0.2	1.808	0.2	0.615	0.1	0.269	0.1	0.221	0.006	52
pHYB^{R582A}	0.77	20	0.731	0.2	1.058	0.1	2.038	0.2	0.288	0.1	0.327	0.1	0.215	0.007	52
pHYB^{R582A}	0.45	20	0.481	0.1	1.385	0.2	2.25	0.2	0.327	0.1	0.365	0.1	0.214	0.007	52
pHYB^{R582A}	0.2	20	0.596	0.1	0.885	0.2	2.365	0.3	0.519	0.1	0.596	0.1	0.194	0.008	52
pHYB^{R582A}	0.07	20	0.558	0.1	0.577	0.1	2.25	0.3	1.019	0.2	0.577	0.1	0.159	0.012	52
pHYB^{R582A}	0.001	20	0.115	0.1	0.212	0.1	2.615	0.3	2.865	0.4	1.654	0.4	0.113	0.007	52
phyB^{Y361F}	Red	20	0.538	0.1	0.942	0.1	1.885	0.2	0.827	0.2	0.923	0.3	0.191	0.008	52
phyB^{Y361F}	0.77	20	0.712	0.1	1.058	0.2	2.135	0.2	0.788	0.1	0.769	0.2	0.196	0.009	52
phyB^{Y361F}	0.45	20	0.442	0.1	1.288	0.2	2.808	0.3	0.654	0.1	0.365	0.1	0.204	0.007	52
phyB^{Y361F}	0.2	20	0.231	0.1	0.788	0.1	4.212	0.4	1.481	0.2	0.654	0.1	0.169	0.006	52
phyB^{Y361F}	0.07	20	0.135	0	0.596	0.1	4.885	0.4	2.519	0.3	1.077	0.3	0.149	0.005	52

phyB^{Y361F}	0.001	20	0.077	0	0.442	0.1	5.538	0.5	3.615	0.5	1.923	0.3	0.131	0.005	52
phyB	Red	25	0.25	0.3	3	1.1	2.25	0.9	0	0	0	0	0.239	0.015	4
phyB	0.77	25	1.5	0.6	2.25	1.3	2.5	1.9	0.75	0.5	1	0.7	0.237	0.035	4
phyB	0.45	25	0	0	1	0.4	3.75	0.8	2.25	1	0.75	0.5	0.156	0.013	4
phyB	0.2	25	0	0	0	0	4.25	0.8	4	1.2	1.5	0.3	0.122	0.01	4
phyB	0.07	25	0	0	0	0	0	0	0.75	0.8	1	0.7	0.023	0.015	4
phyB	0.001	25	0	0	0	0	0	0	0.75	0.8	1.25	0.8	0.023	0.015	4
pHYB^{R582A}	Red	25	0	0	1	0.4	3.75	0.5	1	0.6	1.5	1.5	0.162	0.025	4
pHYB^{R582A}	0.77	25	0.5	0.3	2.5	0.6	2	0.9	0.25	0.3	0.5	0.3	0.237	0.021	4
pHYB^{R582A}	0.45	25	1.5	0.9	2	1.2	1	0.4	0.25	0.3	0.5	0.3	0.271	0.04	4
pHYB^{R582A}	0.2	25	0	0	1.75	0.9	3	0.6	0	0	0	0	0.21	0.012	4
pHYB^{R582A}	0.07	25	0.25	0.3	0.75	0.5	2.5	0.6	1	0.4	0.75	0.5	0.163	0.016	4
pHYB^{R582A}	0.001	25	0	0	0.25	0.3	4.5	1	0.25	0.3	1.5	1.2	0.16	0.015	4
phyB^{Y361F}	Red	25	0.5	0.3	2	1.1	1.75	1.1	0	0	0.25	0.3	0.245	0.031	4
phyB^{Y361F}	0.77	25	1.5	0.9	1.5	0.3	1.5	0.6	0	0	0.75	0.5	0.241	0.023	4
phyB^{Y361F}	0.45	25	0.5	0.5	1	0	2.5	0.9	0	0	0	0	0.233	0.032	4
phyB^{Y361F}	0.2	25	0.25	0.3	1.5	0.9	3.5	1	0.75	0.5	0.25	0.3	0.197	0.026	4
phyB^{Y361F}	0.07	25	0	0	1.25	0.8	8.75	0.6	3.75	1.4	3.5	1	0.139	0.005	4
phyB^{Y361F}	0.001	25	0.5	0.5	1	0.7	4	0.7	1.25	0.6	0	0	0.187	0.016	4
phyB	Red	30	0.375	0.3	1.625	0.4	3	0.4	0.5	0.3	0.375	0.3	0.202	0.015	8
phyB	0.77	30	0.25	0.2	1.375	0.3	3.5	0.8	0.75	0.4	0.5	0.3	0.184	0.01	8
phyB	0.45	30	0	0	0.625	0.2	3.625	0.5	1.25	0.3	0.875	0.5	0.153	0.011	8
phyB	0.2	30	0	0	0	0	4.625	1.4	2.5	0.5	1.75	0.6	0.103	0.019	8
phyB	0.07	30	0	0	0	0	1.25	0.5	2.875	0.8	1.25	0.3	0.08	0.013	8
phyB	0.001	30	0	0	0	0	0.25	0.3	1.25	0.6	1.75	0.6	0.041	0.011	8
pHYB^{R582A}	Red	30	0	0	0.75	0.5	1.125	0.1	0.5	0.3	0.5	0.3	0.168	0.01	8
pHYB^{R582A}	0.77	30	0	0	0.125	0.1	2	0.5	1.625	0.8	1.875	1.5	0.132	0.019	8
pHYB^{R582A}	0.45	30	0.25	0.2	1.5	0.6	3.25	0.9	0.5	0.2	0.625	0.4	0.192	0.02	8
pHYB^{R582A}	0.2	30	0	0	0.875	0.4	4.125	1.2	1.5	0.7	0.5	0.2	0.152	0.014	8
pHYB^{R582A}	0.07	30	0	0	0	0	1.375	0.4	1.375	0.3	0.875	0.5	0.101	0.019	8
pHYB^{R582A}	0.001	30	0.25	0.3	0.375	0.3	2.25	0.9	2.375	0.8	0.625	0.3	0.133	0.019	8
phyB^{Y361F}	Red	30	0	0	0.5	0.3	3.375	0.5	1.5	0.5	0.5	0.2	0.152	0.01	8
phyB^{Y361F}	0.77	30	0	0	0.25	0.2	4.75	0.6	0.25	0.3	0.375	0.2	0.175	0.007	8
phyB^{Y361F}	0.45	30	0	0	0.25	0.3	3.625	0.7	1.125	0.4	1	0.2	0.139	0.009	8
phyB^{Y361F}	0.2	30	0	0	0.25	0.2	5.25	1.1	1.5	0.8	0.375	0.3	0.153	0.012	8
phyB^{Y361F}	0.07	30	0.125	0.1	0.5	0.4	3	1	0.75	0.4	0.5	0.3	0.129	0.034	8
phyB^{Y361F}	0.001	30	0	0	0	0	2	0.8	0.875	0.3	0.5	0.2	0.108	0.02	8

Table S3. Hypocotyl growth.

Growth during a period of 9 h of light-grown seedlings of the Columbia WT, of transgenic lines expressing phyB, phyB^{Y361F} or phyB^{R582A} in the *phyB* null mutant background (two independent lines per construct), and of the *phyB* null mutant background. Seedlings were transferred 1 h after the beginning of the 4th day to 25 different combinations of light (irradiance) and temperature. N: Number of boxes containing seedlings (approximately 12 seedlings of the same box were averaged before calculations).

Genotype	Irradiance ($\mu mol.m^{-2}.s^{-1}$)	Temperature (ºC)	Hypocotyl elongation (mm/9h)	SE	N (boxes)
Col	1	10	0.26	0.02	6.00
Col	10	10	0.25	0.03	6.00
Col	50	10	0.28	0.04	5.00
Col	100	10	0.23	0.04	4.00
Col	200	10	0.21	0.03	6.00
Col	1	15	0.45	0.03	5.00
Col	10	15	0.37	0.03	4.00
Col	50	15	0.33	0.04	6.00
Col	100	15	0.22	0.02	5.00
Col	200	15	0.24	0.04	6.00
Col	1	20	0.65	0.07	5.00
Col	10	20	0.53	0.08	5.00
Col	50	20	0.39	0.04	6.00
Col	100	20	0.28	0.02	6.00
Col	200	20	0.20	0.03	5.00
Col	1	25	1.03	0.03	6.00
Col	10	25	0.84	0.10	6.00
Col	50	25	0.61	0.04	6.00
Col	100	25	0.32	0.03	5.00
Col	200	25	0.25	0.02	6.00
Col	1	30	1.13	0.12	6.00
Col	10	30	0.95	0.14	4.00
Col	50	30	0.75	0.12	4.00
Col	100	30	0.52	0.09	2.00
Col	200	30	0.48	0.09	4.00
phyB-1	1	10	0.27	0.03	6.00
phyB-1	10	10	0.23	0.04	6.00
phyB-1	50	10	0.21	0.02	6.00
phyB-1	100	10	0.17	0.02	6.00
phyB-1	200	10	0.16	0.02	6.00
phyB-1	1	15	0.37	0.03	6.00
phyB-1	10	15	0.33	0.03	4.00
phyB-1	50	15	0.24	0.03	6.00

phyB-1	100	15	0.25	0.04	5.00
phyB-1	200	15	0.22	0.02	5.00
phyB-1	1	20	0.46	0.04	5.00
phyB-1	10	20	0.44	0.05	6.00
phyB-1	50	20	0.43	0.06	6.00
phyB-1	100	20	0.29	0.02	6.00
phyB-1	200	20	0.19	0.03	6.00
phyB-1	1	25	0.97	0.05	6.00
phyB-1	10	25	0.80	0.15	6.00
phyB-1	50	25	0.48	0.03	6.00
phyB-1	100	25	0.42	0.04	6.00
phyB-1	200	25	0.30	0.02	6.00
phyB-1	1	30	0.99	0.16	4.00
phyB-1	10	30	0.89	0.05	2.00
phyB-1	50	30	0.60	0.09	3.00
phyB-1	100	30	0.68	0.05	3.00
phyB-1	200	30	0.45	0.05	1.00
phyB-2	1	10	0.28	0.05	6.00
phyB-2	10	10	0.27	0.05	5.00
phyB-2	50	10	0.26	0.05	6.00
phyB-2	100	10	0.19	0.04	6.00
phyB-2	200	10	0.24	0.08	6.00
phyB-2	1	15	0.48	0.11	6.00
phyB-2	10	15	0.43	0.08	6.00
phyB-2	50	15	0.36	0.08	6.00
phyB-2	100	15	0.41	0.09	6.00
phyB-2	200	15	0.25	0.04	5.00
phyB-2	1	20	1.16	0.09	5.00
phyB-2	10	20	1.05	0.09	6.00
phyB-2	50	20	0.77	0.09	6.00
phyB-2	100	20	0.66	0.12	6.00
phyB-2	200	20	0.30	0.02	6.00
phyB-2	1	25	0.72	0.07	6.00
phyB-2	10	25	0.67	0.09	6.00
phyB-2	50	25	0.41	0.04	6.00
phyB-2	100	25	0.36	0.03	6.00
phyB-2	200	25	0.24	0.02	6.00
phyB-2	1	30	1.45	0.13	4.00
phyB-2	10	30	1.48	0.17	4.00
phyB-2	50	30	1.30	0.15	4.00
phyB-2	100	30	0.71	0.11	4.00
phyB-2	200	30	-	-	0.00
$phyB^{R582A}$ -1	1	10	0.27	0.03	6.00

phyB^{R582A} -1	10	10	0.18	0.01	6.00
phyB^{R582A} -1	50	10	0.26	0.04	6.00
phyB^{R582A} -1	100	10	0.13	0.02	6.00
phyB^{R582A} -1	200	10	0.18	0.02	5.00
phyB^{R582A} -1	1	15	0.28	0.03	5.00
phyB^{R582A} -1	10	15	0.24	0.03	5.00
phyB^{R582A} -1	50	15	0.29	0.03	6.00
phyB^{R582A} -1	100	15	0.27	0.04	6.00
phyB^{R582A} -1	200	15	0.16	0.01	6.00
phyB^{R582A} -1	1	20	0.52	0.06	5.00
phyB^{R582A} -1	10	20	0.36	0.01	5.00
phyB^{R582A} -1	50	20	0.44	0.07	5.00
phyB^{R582A} -1	100	20	0.29	0.04	4.00
phyB^{R582A} -1	200	20	0.21	0.03	6.00
phyB^{R582A} -1	1	25	0.63	0.09	5.00
phyB^{R582A} -1	10	25	0.59	0.10	6.00
phyB^{R582A} -1	50	25	0.50	0.08	6.00
phyB^{R582A} -1	100	25	0.29	0.03	6.00
phyB^{R582A} -1	200	25	0.24	0.05	6.00
phyB^{R582A} -1	1	30	1.03	0.19	6.00
phyB^{R582A} -1	10	30	0.94	0.14	6.00
phyB^{R582A} -1	50	30	0.69	0.07	4.00
phyB^{R582A} -1	100	30	0.57	0.05	4.00
phyB^{R582A} -1	200	30	0.41	0.06	4.00
phyB^{R582A} -2	1	10	0.26	0.03	6.00
phyB^{R582A} -2	10	10	0.28	0.06	4.00
phyB^{R582A} -2	50	10	0.22	0.05	6.00
phyB^{R582A} -2	100	10	0.20	0.03	5.00
phyB^{R582A} -2	200	10	0.24	0.04	6.00
phyB^{R582A} -2	1	15	0.37	0.07	6.00
phyB^{R582A} -2	10	15	0.28	0.03	5.00
phyB^{R582A} -2	50	15	0.30	0.04	6.00
phyB^{R582A} -2	100	15	0.30	0.06	6.00
phyB^{R582A} -2	200	15	0.24	0.02	6.00
phyB^{R582A} -2	1	20	0.53	0.05	5.00
phyB^{R582A} -2	10	20	0.38	0.02	6.00
phyB^{R582A} -2	50	20	0.39	0.04	5.00

phyB^{R582A} -2	100	20	0.27	0.04	6.00
phyB^{R582A} -2	200	20	0.25	0.05	4.00
phyB^{R582A} -2	1	25	1.13	0.06	6.00
phyB^{R582A} -2	10	25	0.78	0.07	6.00
phyB^{R582A} -2	50	25	0.51	0.09	5.00
phyB^{R582A} -2	100	25	0.41	0.06	6.00
phyB^{R582A} -2	200	25	0.36	0.04	6.00
phyB^{R582A} -2	1	30	0.62	0.03	3.00
phyB^{R582A} -2	10	30	0.91	0.21	4.00
phyB^{R582A} -2	50	30	0.77	0.07	4.00
phyB^{R582A} -2	100	30	0.53	0.14	2.00
phyB^{R582A} -2	200	30	0.40	0.11	3.00
phyB^{Y361F} -1	1	10	0.20	0.02	6.00
phyB^{Y361F} -1	10	10	0.16	0.03	6.00
phyB^{Y361F} -1	50	10	0.16	0.03	6.00
phyB^{Y361F} -1	100	10	0.15	0.03	5.00
phyB^{Y361F} -1	200	10	0.23	0.04	5.00
phyB^{Y361F} -1	1	15	0.29	0.06	5.00
phyB^{Y361F} -1	10	15	0.24	0.03	6.00
phyB^{Y361F} -1	50	15	0.26	0.03	6.00
phyB^{Y361F} -1	100	15	0.26	0.05	6.00
phyB^{Y361F} -1	200	15	0.29	0.06	5.00
phyB^{Y361F} -1	1	20	0.36	0.04	5.00
phyB^{Y361F} -1	10	20	0.37	0.04	6.00
phyB^{Y361F} -1	50	20	0.34	0.03	5.00
phyB^{Y361F} -1	100	20	0.28	0.02	6.00
phyB^{Y361F} -1	200	20	0.27	0.04	6.00
phyB^{Y361F} -1	1	25	0.64	0.07	6.00
phyB^{Y361F} -1	10	25	0.48	0.05	6.00
phyB^{Y361F} -1	50	25	0.39	0.05	6.00
phyB^{Y361F} -1	100	25	0.32	0.02	6.00
phyB^{Y361F} -1	200	25	0.27	0.03	6.00
phyB^{Y361F} -1	1	30	0.56	0.14	5.00
phyB^{Y361F} -1	10	30	0.54	0.10	4.00
phyB^{Y361F} -1	50	30	0.41	0.03	4.00
phyB^{Y361F} -1	100	30	0.42	0.08	3.00
phyB^{Y361F} -1	200	30	0.86	0.53	4.00

phyB^{Y361F}-2	1	10	0.14	0.02	6.00
phyB^{Y361F}-2	10	10	0.17	0.03	4.00
phyB^{Y361F}-2	50	10	0.13	0.01	6.00
phyB^{Y361F}-2	100	10	0.11	0.01	6.00
phyB^{Y361F}-2	200	10	0.11	0.01	6.00
phyB^{Y361F}-2	1	15	0.22	0.04	6.00
phyB^{Y361F}-2	10	15	0.30	0.05	5.00
phyB^{Y361F}-2	50	15	0.24	0.02	6.00
phyB^{Y361F}-2	100	15	0.22	0.04	6.00
phyB^{Y361F}-2	200	15	0.23	0.03	5.00
phyB^{Y361F}-2	1	20	0.29	0.03	5.00
phyB^{Y361F}-2	10	20	0.27	0.05	6.00
phyB^{Y361F}-2	50	20	0.34	0.04	6.00
phyB^{Y361F}-2	100	20	0.24	0.01	6.00
phyB^{Y361F}-2	200	20	0.16	0.03	5.00
phyB^{Y361F}-2	1	25	0.61	0.10	6.00
phyB^{Y361F}-2	10	25	0.58	0.08	6.00
phyB^{Y361F}-2	50	25	0.43	0.05	6.00
phyB^{Y361F}-2	100	25	0.31	0.05	6.00
phyB^{Y361F}-2	200	25	0.18	0.01	6.00
phyB^{Y361F}-2	1	30	0.77	0.16	5.00
phyB^{Y361F}-2	10	30	0.76	0.11	5.00
phyB^{Y361F}-2	50	30	0.65	0.24	3.00
phyB^{Y361F}-2	100	30	0.41	0.10	4.00
phyB^{Y361F}-2	200	30	0.29	0.02	1.00
phyB	1	10	0.49	0.04	11.00
phyB	10	10	0.39	0.02	11.00
phyB	50	10	0.46	0.07	11.00
phyB	100	10	0.31	0.02	11.00
phyB	200	10	0.30	0.03	12.00
phyB	1	15	0.60	0.04	8.00
phyB	10	15	0.51	0.04	9.00
phyB	50	15	0.45	0.04	9.00
phyB	100	15	0.44	0.06	8.00
phyB	200	15	0.36	0.03	7.00
phyB	1	20	1.39	0.15	11.00
phyB	10	20	1.24	0.09	11.00
phyB	50	20	0.96	0.06	12.00
phyB	100	20	0.67	0.10	12.00

phyB	200	20	0.33	0.03	9.00
phyB	1	25	1.69	0.06	12.00
phyB	10	25	1.28	0.08	11.00
phyB	50	25	0.81	0.05	11.00
phyB	100	25	0.70	0.04	10.00
phyB	200	25	0.40	0.04	11.00
phyB	1	30	1.94	0.11	7.00
phyB	10	30	1.95	0.16	7.00
phyB	50	30	1.68	0.29	5.00
phyB	100	30	1.36	0.18	4.00
phyB	200	30	0.69	0.08	5.00

Table S4. Statistical analysis of all possible interactions among the terms that reduce hypocotyl growth.

We analyzed seven variants of the model presented in equation (4), which includes the effects of D2, temperature and irradiance (other photoreceptors). These variants differ in the interaction terms that they include. Only the interaction between D2 and temperature resulted significant.

Interaction	Estimated value	*P*	R^2
(1/T-1/30) * D2	66.56	<0.0001	0.19
(1/T-1/30) * Irradiance	-0.0039	0.95	
Irradiance * D2	-0.01	0.17	
(1/T-1/30) * D2	69.05	<0.0001	0.18
(1/T-1/30) * Irradiance	-0.05	0.34	
(1/T-1/30) * Irradiance	0.17	0.0013	0.05
Irradiance * D2	-0.01	0.0335	
(1/T-1/30) * D2	66.14	<0.0001	0.19
Irradiance * D2	-0.01	0.096	
(1/T-1/30) * D2	**63.24**	**<0.0001**	**0.18**
Irradiance * D2	-0.001	0.67	0.0009
(1/T-1/30) * Irradiance	0.11	0.014	0.03